Acta Mech 228, 3003–3017 (2017)
DOI 10.1007/s00707-017-1871-y

ORIGINAL PAPER

Gökhan Adıyaman · Erdal Öner · Ahmet Birinci

Continuous and discontinuous contact problem of a functionally graded layer resting on a rigid foundation

Received: 17 October 2016 / Revised: 19 April 2017 / Published online: 19 May 2017

Abstract In this study, the continuous and discontinuous contact problem of a functionally graded (FG) layer resting on a rigid foundation is considered. The top of the FG layer is subjected to normal tractions over a finite segment. The graded layer is modeled as a non-homogenous medium with a constant Poissons' ratio and exponentially varying shear modules and density. For continuous contact, the problem was solved analytically using plane elasticity and integral transform techniques. The critical load that causes first separation and contact pressures is investigated for various material properties and loadings. The problem reduced to a singular integral equation using plane elasticity and integral transform techniques in case of discontinuous contact. The obtained singular integral equation is solved numerically using Gauss–Jacobi integral formulation, and an iterative scheme is employed to obtain the correct separation distance. The separation distance and contact pressures between the FG layer and the foundation are analyzed for various material properties and loading. The results are shown in Tables and Figures. It is seen that decreasing stiffness and density at the top of the layer result in an increment in both critical load in case of continuous contact and separation distance in case of discontinuous contact.

1 Introduction

In problems in which body forces are neglected, after the application of the load, the contact area between the layer and the substrate diminish to a finite size independent of the magnitude of the applied load. However, in reality, it is expected that the separation depends on the applied load and the layer will remain in contact with the substrate at some point because of gravity.

Civelek and Erdogan [1] studied the frictionless contact problem of an elastic layer under gravity. Civelek et al.[2] studied the interface separation for an elastic layer loaded by a rigid stamp. Continuous and discontinuous contact problems for strips on an elastic semi-infinite plane were investigated by Cakiroglu and Cakiroglu [3]. Birinci and Erdol [4] studied a frictionless contact problem for two elastic layers with vertical body forces supported by a Winkler foundation. Oner and Birinci [5] studied the continuous contact problem for two elastic layers resting on an elastic half-infinite plane. An analysis of continuous and discontinuous cases of a contact problem using analytical method and FEM was performed by Birinci et al [6].

Parallel to developments in sciences, new materials such as functionally graded materials (FGMs) in which material properties vary smoothly along a spatial direction are developed as an alternative to homogeneous

G. Adıyaman (✉) · A. Birinci
Department of Civil Engineering, Karadeniz Technical University, 61080 Trabzon, Turkey
E-mail: gadiyaman@ktu.edu.tr
Tel.: +904623772606

E. Öner
Department of Civil Engineering, Bayburt University, 69000 Bayburt, Turkey

materials. These materials are used in various applications, including ball and roller bearings, gears, cutting edges, gas turbines, electromagnetic engineering and space vehicles, mostly to provide abrasion resistance and high-temperature endurance. Such a wide range of applications has resulted in the inevitable use of FGMs in contact mechanics. Several studies have examined the contact problems of layers made from FGMs.

Giannakopoulos and Pallot [7] examined the two-dimensional contact of a rigid cylinder on an elastic graded substrate. Guler and Erdogan [8,9] studied the fracture initiation in graded coatings under sliding contact loading and the contact problem for two deformable solids with FGM coatings. A multilayered model for sliding frictional contact analysis of functionally graded materials (FGMs) with arbitrarily varying shear modulus under plane strain-state deformation has been developed by Ke and Wang [10]. Barik et al. [11] studied the stationary plane contact of a functionally graded heat conducting punch and a rigid insulated half-space. The frictionless contact problem of a functionally graded piezoelectric layered half-plane in plane strain state under the action of a rigid flat or cylindrical punch was examined by Ke et al. [12]. Sliding frictional contact between a rigid punch and a laterally graded elastic medium was studied by Dag et al. [13]. Comez [14] considered a contact problem for a functionally graded layer loaded by means of a rigid stamp and supported by a Winkler foundation. Çömez [15] also solved a contact problem for a functionally graded layer indented by a moving punch. The axisymmetric contact problem on the indentation of a hot circular punch into an arbitrarily nonhomogeneous half-space was considered by Krenev et al. [16]. Wang et al. [17] investigated an efficient method for solving three-dimensional fretting contact problems involving multilayered or functionally graded materials. Frictional receding contact analysis of a layer on a half-plane subjected to semi-infinite surface pressure was studied by Parel and Hills [18]. Ma et al. [19] investigated the frictional contact problem between a functionally graded magnetoelectroelastic layer and a rigid conducting flat punch with frictional heat generation.

A receding contact plane problem for a functionally graded layer pressed against a homogeneous half-space was analyzed by El-Borgi et al. [20]. Rhimi et al. [21,22] considered the axisymmetric problem of a frictionless receding contact between an elastic functionally graded layer and a homogeneous half-space when the two bodies were pressed together, and double receding contact between a rigid stamp of axisymmetric profile, an elastic functionally graded layer and a homogeneous half-space. The two-dimensional frictionless contact problem of a coating structure consisting of a surface coating, a functionally graded layer and a substrate under a rigid cylindrical punch was investigated by Yang and Ke [23]. Chen and Chen [24] studied the contact behaviors of a graded layer resting on a homogeneous half-space and pressed by a rigid stamp. The plane problem of a frictional receding contact formed between an elastic functionally graded layer and a homogeneous half-space, when they were pressed against each other, was investigated by El-Borgi et al. [25]. Yan and Li [26] considered the double receding contact plane problem between a functionally graded layer and an elastic layer. A three-dimensional problem of elasticity of normal and tangential loading of the surface of the functionally graded coated half-space was examined by Kulchytsky-Zhyhailo and Bajkowski [27]. Alinia et al. [28] considered the fully coupled contact problem between a rigid cylinder and a functionally graded coating bonded to a homogeneous substrate system under plane strain and generalized plane stress sliding conditions.

An examination of the related literature shows that studies involving layers or coatings with body forces have consisted of homogeneous materials, whereas studies involving FG layers or coating have neglected body forces. Therefore, this study aims to solve the continuous and discontinuous contact problem of an FG layer resting on a rigid foundation by taking into account the body force of the FG layer. Further, the calculations are made under the assumption that the FG layer is isotropic and the shear modulus and mass density exponentially vary along the direction of the layer's thickness.

2 Formulation of the problem

As shown in Fig. 1, consider the symmetric plane strain problem consisting of an infinitely long functionally graded (FG) layer of thickness h resting on a rigid foundation. Poisson's ratio ν is taken as constant; the shear modulus μ and the density ρ depend on the y-coordinate only as follows:

$$\mu(y) = \mu_0 \exp(\beta y), \qquad 0 \le y \le h, \tag{1.1}$$

$$\rho(y) = \rho_0 \exp(\alpha y), \qquad 0 \le y \le h, \tag{1.2}$$

where μ_0 and ρ_0 are the shear modulus and the density of the graded layer at $y = 0$; β and α are the non-homogeneity parameters controlling the variation of the shear moduli and the density in the graded layer, respectively.

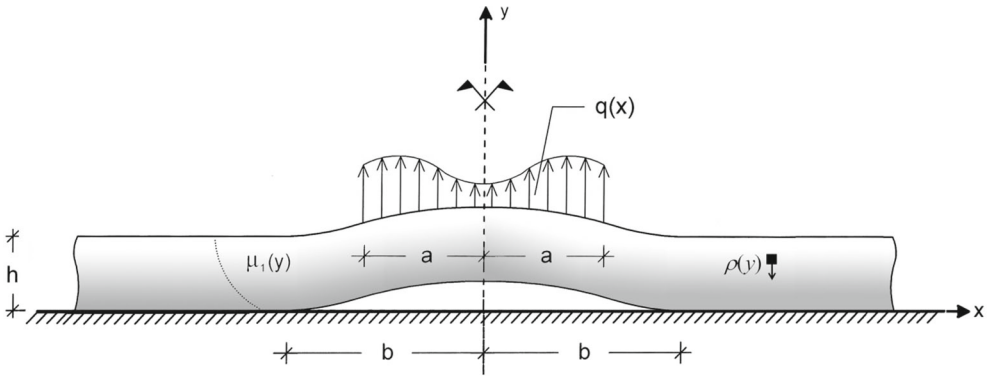

Fig. 1 Geometry and loading of the contact problem

The top of the layer is subjected to a distributed load $q(x)$ over the segment $|x| \leq a$. It is assumed that the contact surfaces are frictionless and $x = 0$ is the plane of symmetry with respect to external loads as well as geometry, for simplicity. Clearly, it is sufficient to consider one half (i.e., $x \geq 0$) of the medium only.

Assuming that the FG layer is isotropic at every point, equilibrium equations, the strain-displacement relationships, and the linear elastic stress–strain law, respectively, are given by:

$$\frac{\partial \sigma_x}{\partial x} + \frac{\tau_{xy}}{\partial y} = 0, \qquad \frac{\partial \tau_{xy}}{\partial x} + \frac{\partial \sigma_y}{\partial y} - \rho g = 0, \tag{2.1,2}$$

$$\varepsilon_{xx} = \frac{\partial u}{\partial x}, \qquad \varepsilon_{yy} = \frac{\partial v}{\partial y}, \qquad \varepsilon_{xy} = \frac{1}{2}\left(\frac{\partial u}{\partial y} + \frac{\partial v}{\partial x}\right), \tag{3.1–3}$$

$$\sigma_x = \frac{\mu_1}{\kappa - 1}\left[(1+\kappa)\varepsilon_{xx} + (3-\kappa)\varepsilon_{yy}\right], \tag{4.1}$$

$$\sigma_y = \frac{\mu_1}{\kappa - 1}\left[(3-\kappa)\varepsilon_{xx} + (1+\kappa)\varepsilon_{yy}\right], \tag{4.2}$$

$$\tau_{xy} = 2\mu\varepsilon_{xy} \tag{4.3}$$

where u and v are the x and y components of the displacement field, respectively; σ_x, σ_y and τ_{xy} are the components of the stress field in the same coordinate system; ε_x, ε_y, and ε_{xy} are the corresponding components of the strain field; κ is a material property defined as $\kappa = 3-4\nu$ for plane strain problems; and g is gravitational acceleration. Combining Eqs. (1)–(4), the following two-dimensional Navier's equations are obtained:

$$(\kappa+1)\frac{\partial^2 u}{\partial x^2} + (\kappa-1)\frac{\partial^2 u}{\partial y^2} + 2\frac{\partial^2 v}{\partial x \partial y} + \beta(\kappa-1)\frac{\partial u}{\partial y} + B(\kappa-1)\frac{\partial v}{\partial x} = 0, \tag{5.1}$$

$$(\kappa-1)\frac{\partial^2 v}{\partial x^2} + (\kappa+1)\frac{\partial^2 v}{\partial y^2} + 2\frac{\partial^2 u}{\partial x \partial y} + \beta(3-\kappa)\frac{\partial u}{\partial x} + \beta(\kappa+1)\frac{\partial v}{\partial y} = \rho_m e^{(\beta-\alpha)y}. \tag{5.2}$$

in which ρ_m is defined as follows:

$$\rho_m = \frac{\kappa - 1}{\mu_0}\rho_0 g.$$

The solution of (5) can be given as

$$u = u_p + u_h, \tag{6.1}$$

$$v = v_p + v_h \tag{6.2}$$

where subscripts p and h represent the particular and homogeneous solution, respectively.

For the particular solution, assuming displacement components $u_p = u_p(x)$ and $v_p = v_p(y)$, Eq. (5) yields

$$(\kappa+1)\frac{\partial^2 u}{\partial x^2} = 0, \tag{7.1}$$

$$(\kappa+1)\frac{\partial^2 v}{\partial y^2}+\beta(3-\kappa)\frac{\partial u}{\partial x}+\beta(\kappa+1)\frac{\partial v}{\partial y}=\rho_m e^{(\beta-\alpha)y}, \tag{7.2}$$

and the displacements may be expressed as

$$u_p = A_1 x + A_2, \tag{8.1}$$

$$v_p = C_1 e^{-\beta y}+\frac{\rho_m e^{(\alpha-\beta)y}}{\alpha(\alpha-\beta)(\kappa+1)}+\frac{(1-\beta y)(3-\kappa)A_1-C_2}{\beta(\kappa+1)} \tag{8.2}$$

in which A_i and C_i $(i = 1, 2)$ are unknown constants and can be found applying the following boundary conditions (given in "Appendix A"):

$$u_p(0, y) = 0, \qquad v_p(x, 0) = 0, \tag{9.1,2}$$

$$\sigma_{y_p}(x, 0) = -\frac{\rho_0 g}{\alpha}\left(e^{\alpha h}-1\right), \qquad \int_0^h \sigma_{x_p} dy = 0. \tag{9.3,4}$$

The particular part of the stress component σ_{y_p} is obtained as follows:

$$\sigma_{y_p}(y) = -\frac{\rho_0 g}{\alpha}\left(e^{\alpha h}-e^{\alpha y}\right). \tag{10}$$

In case of homogeneous solution, using symmetry considerations and Fourier transforms, the displacement components for the FG layer may be written as:

$$u_h(x, y) = \frac{2}{\pi}\int_0^\infty \phi(\xi, y)\sin(\xi x)d\xi, \qquad v_h(x, y) = \frac{2}{\pi}\int_0^\infty \psi(\xi, y)\cos(\xi x)d\xi \tag{11.1,2}$$

where $\phi(\xi, y)$ and $\psi(\xi, y)$ are the Fourier sine and Fourier cosine transforms of u and v with respect to the x-coordinate, respectively. Substituting Eqs. (11.1,2) into Navier's equations (5), the following ordinary differential equations are obtained:

$$-(\kappa_1+1)\xi^2\phi+(\kappa_1-1)\frac{d^2\phi}{d^2}-2\xi\frac{d\psi}{dy}+\beta(\kappa_1-1)\left[\frac{d\phi}{dy}-\xi\psi\right]=0, \tag{12.1}$$

$$-(\kappa_1-1)\xi^2\psi+(\kappa_1+1)\frac{d^2\psi}{dy^2}+2\xi\frac{d\phi}{dy}+\beta\left[(3-\kappa_1)\xi\phi+(\kappa_1+1)\frac{d\psi}{dy}\right]=0 \tag{12.2}$$

where

$$\phi=\sum_{j=1}^{4} F_j \exp\left(n_j y\right), \qquad \psi=\sum_{j=1}^{4} F_j m_j \exp\left(n_j y\right). \tag{13.1,2}$$

The unknown functions F_j $(j = 1, 2, 3, 4)$ are determined from the boundary conditions, and $n_1, \ldots, n_4$ are the four complex roots of the characteristic equation associated with Eqs. (12.1,2), which may be written as:

$$n_j^4+2\beta n_j^3+(\beta^2-2\xi^2)n_j^2-2\xi^2\beta n_j+\xi^2\left(\xi^2+\beta^2\frac{3-\kappa_1}{\kappa_1+1}\right)=0. \tag{14}$$

The roots of Eq. (14) are obtained:

$$n_1=-\frac{1}{2}\left(\beta+\sqrt{4\xi^2+\beta^2-4\xi\beta i\sqrt{\frac{3-\kappa_1}{\kappa_1+1}}}\right), \qquad n_2=-\frac{1}{2}\left(\beta-\sqrt{4\xi^2+\beta^2-4\xi\beta i\sqrt{\frac{3-\kappa_1}{\kappa_1+1}}}\right), \tag{15.1,2}$$

$$n_3 = -\frac{1}{2}\left(\beta + \sqrt{4\xi^2 + \beta^2 + 4\xi\beta i\sqrt{\frac{3-\kappa_1}{\kappa_1+1}}}\right), \qquad n_4 = -\frac{1}{2}\left(\beta - \sqrt{4\xi^2 + \beta^2 + 4\xi\beta i\sqrt{\frac{3-\kappa_1}{\kappa_1+1}}}\right), \tag{15.3,4}$$

The known function m_j in Eq. (13.2) may be expressed as follows:

$$m_j = \frac{\left(3\beta + 2n_j - \beta\kappa_1\right)\left[n_j\left(\beta + n_j\right)(\kappa_1+1) - \xi^2(\kappa_1+3)\right]}{\xi\left[4\xi^2 - \beta^2(\kappa_1-3)(\kappa_1+1)\right]}, \qquad (j = 1, 2, 3, 4). \tag{16}$$

Substituting Eqs. (11.1,2) and (13.1,2) into Eqs. (4), the stress and displacement fields of interest for the graded layer are obtained:

$$\sigma_{y_h} = \frac{2\mu_0 \exp(\beta y)}{\pi(\kappa_1 - 1)} \int_0^\infty \sum_{j=1}^4 F_j S_j \exp\left(n_j y\right) \cos(\xi x)\, d\xi, \tag{17.1}$$

$$\tau_{xy_h} = \frac{2\mu_0 \exp(\beta y)}{\pi} \int_0^\infty \sum_{j=1}^4 F_j T_j \exp\left(n_j y\right) \sin(\xi x)\, d\xi, \tag{17.2}$$

$$v_h = \frac{2}{\pi} \int_0^\infty \sum_{j=1}^4 F_j m_j \exp\left(n_j y\right) \cos(\xi x)\, d\xi, \tag{18}$$

in which the known functions S_j and $T_j (j = 1, 2, 3, 4)$ are given by:

$$S_j = (3 - \kappa_1)\xi + (\kappa_1 + 1) m_j n_j, \qquad T_j = n_j - \xi m_j. \tag{19.1,2}$$

3 Solution of the problem

The solution of the problem is carried out in case of continuous contact and discontinuous contact separately.

3.1 In case of continuous contact

If the load is sufficiently small, then the contact between the FG layer and the rigid foundation becomes continuous, and the boundary conditions can be defined as follows:

$$\sigma_y(x, h) = q(x)H(a - |x|), \qquad \tau_{xy}(x, h) = 0, \qquad 0 \le x < \infty, \tag{19.1,2}$$

$$v(x, 0) = 0, \qquad \tau_{xy}(x, 0) = 0, \qquad 0 \le x < \infty \tag{19.3,4}$$

where H is the Heaviside function.

Applying boundary conditions (19.1–4) to stress and displacement fields (17,18), the following linear algebraic system of equations is obtained:

$$\begin{bmatrix} S_1 \exp(n_1 h) & S_2 \exp(n_2 h) & S_3 \exp(n_3 h) & S_4 \exp(n_4 h) \\ T_1 \exp(n_1 h) & T_1 \exp(n_1 h) & T_1 \exp(n_1 h) & T_1 \exp(n_1 h) \\ T_1 & T_2 & T_3 & T_4 \\ m_1 & m_2 & m_3 & m_4 \end{bmatrix} \begin{Bmatrix} F_1 \\ F_2 \\ F_3 \\ F_4 \end{Bmatrix} = \begin{Bmatrix} Q \\ 0 \\ 0 \\ 0 \end{Bmatrix} \tag{20}$$

where Q is a known function defined as:

$$Q = \frac{\kappa - 1}{\mu_0 \exp(\beta h)} \int_0^\infty q(x)H(a - x)\cos\xi x dx. \tag{21}$$

The unknown functions F_j $(j = 1, 2, 3, 4)$ may be obtained in terms of Q solving Eq. (20) analytically and can be expressed as:

$$F_j = \frac{F_{j1}}{\Delta F} Q \tag{22}$$

where F_{j1} $(j = 1, 2, 3, 4)$ and ΔF are shown in "Appendix A." Assuming $q(x)$ as a uniformly distributed load,

$$q(x) = q_0, \tag{23}$$

Q becomes as follows:

$$Q = \frac{\kappa - 1}{\mu_0 \exp(\beta h)} q_0 \frac{\sin \xi a}{\xi}. \tag{24}$$

Substituting Eqs. (10, 17.1, 22, 24) into the stress field of interest, the following expression is obtained:

$$\frac{\sigma_y}{\rho_0 g h} = \frac{2 \exp(\beta(y-h))}{\pi\,(a/h)} \lambda \int_0^\infty \frac{1}{\xi \Delta F} \sum_1^4 \left[F_{j1} S_1 \exp(n_j y)\right] \sin \xi a \cos \xi x d\xi - \frac{\exp(\alpha h) - \exp(\alpha y)}{\alpha h} \tag{25}$$

in which λ is a dimensionless load factor parameter defined as

$$\lambda = \frac{P}{\rho_0 g h^2} \tag{26}$$

where P is the resultant force of the distributed load in case of uniformly distributed load,

$$P = \int_{-a}^{a} q(x) dx = 2 q_0 a. \tag{27}$$

The separation of the FG layer occurs at $x = 0$, the symmetry axis, and the critical load, λ_{cr}, that cause first separation can be found equating Eq. (25) to zero at $y = 0$,

$$\frac{1}{\lambda_{cr}} = \frac{\alpha h}{\exp(\alpha h) - 1} \frac{2 \exp(-\beta h)}{\pi\,(a/h)} \int_0^\infty \frac{1}{\xi \Delta F} \sum_1^4 \left[F_{j1} S_1 \exp(n_j y)\right] \sin \xi a \cos \xi x d\xi. \tag{28}$$

3.2 In case of discontinuous contact

Since the contact surface cannot carry tensile tractions for $\lambda > \lambda_{cr}$, there occurs a separation between the FG layer and the rigid foundation in the neighborhood of $x = 0$ symmetry axis at $y = 0$. Assuming that the separation region is described by $-b < x < b$, the boundary conditions can be defined as follows:

$$\sigma_y(x, h) = q(x) H(a - |x|), \qquad \tau_{xy}(x, h) = 0, \qquad 0 \le x < \infty, \tag{29.1,2}$$

$$\frac{\partial v(x, 0)}{\partial x} = f(x), \qquad \tau_{xy}(x, 0) = 0, \qquad 0 \le x < \infty, \tag{29.3,4}$$

$$\sigma_y(x, 0) = 0 \qquad -b < x < b \tag{29.5}$$

in which $f(x)$ is the derivative of the separation distance between the layer and the rigid foundation with respect to x, and single-valuedness for vertical displacement $v(x, 0)$ requires that $f(x)$ satisfies the following condition:

$$\int_{-b}^{b} f(x) dx = 0. \tag{30}$$

Applying boundary conditions (29.1–4) to stress and displacement fields (17, 18), the following linear algebraic system of equations is obtained:

$$\begin{bmatrix} S_1\exp(n_1h) & S_2\exp(n_2h) & S_3\exp(n_3h) & S_4\exp(n_4h) \\ T_1\exp(n_1h) & T_1\exp(n_1h) & T_1\exp(n_1h) & T_1\exp(n_1h) \\ T_1 & T_2 & T_3 & T_4 \\ -\xi m_1 & -\xi m_2 & -\xi m_3 & -\xi m_4 \end{bmatrix} \begin{Bmatrix} F_1 \\ F_2 \\ F_3 \\ F_4 \end{Bmatrix} = \begin{Bmatrix} Q \\ 0 \\ 0 \\ F \end{Bmatrix} \tag{31}$$

where F is a known function defined as:

$$F = \int_0^\infty f(x)\sin\xi x dx = \int_0^b f(t)\sin\xi t dt. \tag{32}$$

The new values for the unknown functions F_j ($j = 1, 2, 3, 4$) may be obtained in terms of Q and F solving Eq. (31) analytically and can be expressed as:

$$F_j = \frac{F_{j1}}{\Delta F}F + \frac{F_{j2}}{\Delta F}\xi Q \tag{33}$$

where F_{j1}, F_{j2} ($j = 1, 2, 3, 4$) and ΔF are shown in "Appendix A." Substituting (10, 17.1, 33) into the stress field of interest, the following expression is obtained:

$$\sigma_y = \frac{2\mu_0\exp(\beta y)}{\pi(\kappa-1)}\int_0^\infty \frac{1}{\Delta F}\sum_1^4 \left[F_{j1}F + F_{j2}\xi Q\right]S_j\exp(n_j y)\cos\xi x d\xi - \frac{\rho_0 g\left[\exp(\alpha h) - \exp(\alpha y)\right]}{\alpha}. \tag{34}$$

Applying the unused boundary condition (29.5), substituting F and Q, and using the anti-symmetry condition $f(x) = -f(x)$, the following singular integral equation is obtained assuming that the load is uniformly distributed:

$$\frac{4\mu_0}{\kappa+1}\left[\frac{1}{\pi}\int_{-b}^{b} f(t)\frac{1}{t-x}dt + \frac{1}{\pi}\int_{-b}^{b} f(t)K_1 dt\right] + \rho_0 gh\left[\frac{1}{a/h\exp(\beta h)}\frac{\lambda}{\pi}K_2 - \frac{\exp(\alpha h)-1}{\alpha h}\right] = 0 \tag{35}$$

in which K_1 and K_2 are described in "Appendix A."

4 Numerical solution

Using the following dimensionless quantities, the numerical solution of the continuous and discontinuous problem can be simplified,

$$t = sb, \qquad dt = bds, \qquad x = rb, \qquad w = \xi h, \qquad dw = hd\xi, \tag{36,1–5}$$

$$\phi(s) = \frac{4\mu_0}{(\kappa+1)}f(t). \tag{37}$$

The expressions for the critical load factor (28), the singular integral equation (35), and the single-valuedness condition (30) become:

$$\frac{1}{\lambda_{cr}} = \frac{\alpha h}{\exp(\alpha h)-1}\frac{2\exp(-\beta h)}{\pi(a/h)}\int_0^\infty \frac{1}{w\Delta F}\sum_1^4\left[F_{j1}S_1\exp(n_j y)\right]\sin\left(w\frac{a}{h}\right)\cos\left(w\frac{x}{d}\right)dw, \tag{38}$$

$$\frac{1}{\pi}\int_{-1}^{1}\phi(s)\left[\frac{1}{t-x} + \frac{b}{h}k_1\right]ds + \frac{1}{a/h\exp(\beta h)}\frac{\lambda}{\pi}k_2 - \frac{\exp(\alpha h)-1}{\alpha h} = 0, \tag{39}$$

$$k_1(r,s) = hK_1(r,s), \qquad k_2(r,s) = hK_2(r,s), \tag{40.1,2}$$

$$\frac{b}{h}\int_{-1}^{1}\phi(s)ds = 0. \tag{41}$$

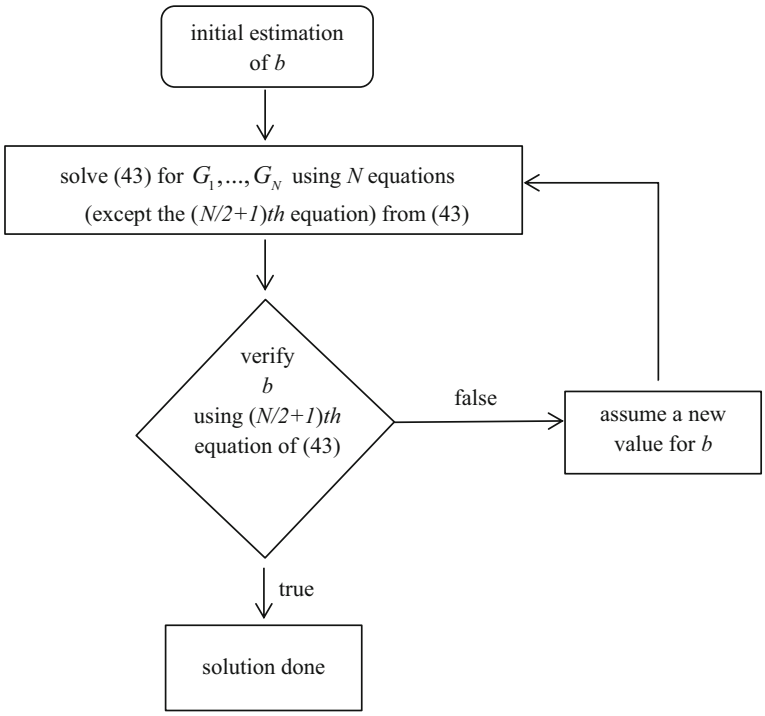

Fig. 2 Flowchart of the iterative algorithm

Since $f(t)$ or $\phi(s)$ is an odd function, *i.e.*, $f(t) = -f(t)$, (41) is automatically satisfied. In addition, one may notice that because of the smooth contact at the points $s = -1$ and $s = 1$, the function $\phi(s)$ in Eq. (39) equals zero at both ends. Hence, the index of the integral equation is -1, and the solution may be sought as described by Erdogan et al. [29]:

$$\phi(s) = (1-s^2)^{1/2} G(s), \qquad W(s) = \frac{1-s^2}{N+1}, \qquad -1 \le s \le 1. \tag{42.1,2}$$

Using appropriate Gauss–Jacobi integration formulas, the solution of Eq. (39) may be expressed as a system of algebraic equations as given below,

$$\sum_{j=1}^{N} \frac{1-s_j^2}{N+1} G(s_j) \left[\frac{1}{s_j - r_i} + \frac{b}{h} k_1(r_i, s_j) \right] = \frac{\exp(\alpha h) - 1}{\alpha h} - \frac{1}{a/h \exp(\beta h)} \frac{\lambda}{\pi h} k_2(r_i), \quad (i = 1, ..., N+1), \tag{43}$$

where r_i and s_k are shown in "Appendix A."

The system of algebraic equations (43) consists of $(N+1)$ equations with $(N+1)$ unknowns, namely $G_1, \ldots, G_N$, and b. When analyzed, it is observed that the system of equations given by (43) is nonlinear in terms of the variable b, and an iterative procedure given as a flowchart in Fig. 2 can be used to find the unknowns. As it is seen from Fig. 2, firstly an initial estimate of the variable b is assumed, and choosing (N) equations (except the $(N/2+1)th$ equation) from (43), the solution is found for the unknowns $G_1, \ldots, G_N$. The unused equation of (43), *i.e.*, $(N/2+1)th$ equation, b should be verified using calculated $G_1, \ldots, G_N$ values. If the assumed variable b satisfies this equation within an acceptable error, *i.e.*, accuracy which is the difference between the left-hand side and right-hand side of the $(N/2+1)th$ equation, it is assumed that the correct values of $G_1, \ldots, G_N$, and b are obtained. Otherwise, a new value for b is assigned for the next iteration, and the procedure continues.

5 Numerical results

The geometry and loading of the problem are given in Fig. 1. The load applied on the FG layer, i.e., $q(x)$, is a uniformly distributed load with $a/h = 0.01,\ 0.5,\ 1.0,\ 2.0$. The load can be considered as concentrated force for $a/h = 0.01$.

Table 1 The comparison of λ_{cr} in case of continuous contact and b/h in case of the discontinuous case ($a/h = 0.01$)

Study	Continuous contact, λ_{cr}	Discontinuous, b/h^*		
		$\lambda = 1.2$	$\lambda = 2.0$	$\lambda = 4.0$
Civelek and Erdogan [1]	1.088	0.28	0.96	2.35
This study	1.088625	0.287155	0.970928	2.387936

* b/h values are read from the enlarged figures

Table 2 The variation of λ_{cr} for the various β and α in case of continuous contact ($a/h = 0.01$, $\kappa = 2.0$)

Parameters	$\alpha = -1.0$	$\alpha = -0.5$	$\alpha = 0.001$	$\alpha = 0.5$	$\alpha = 1.0$
$\beta = -1.0$	0.660946	0.822824	1.046125	1.356608	1.796639
$\beta = -0.5$	0.672888	0.837691	1.065026	1.381119	1.829100
$\beta = 0.001$	0.687798	0.856253	1.088625	1.411723	1.869630
$\beta = 0.5$	0.705887	0.878772	1.117255	1.448850	1.918800
$\beta = 1.0$	0.727571	0.905767	1.151576	1.493357	1.977743

Table 3 The variation of the λ_{cr} for the various a/h, β and α in case of continuous contact ($\kappa = 2.0$)

Parameters	$\beta = -1.0$ $\alpha = -1.0$	$\beta = -1.0$ $\alpha = 1.0$	$\beta = 0.001$ $\alpha = 0.001$	$\beta = 1.0$ $\alpha = -1.0$	$\beta = 1.0$ $\alpha = 1.0$
$a/h = 0.01$	0.660946	1.796639	1.088625	0.727571	1.977743
$a/h = 0.1$	0.667269	1.813826	1.097933	0.732991	1.992477
$a/h = 0.5$	0.817603	2.222475	1.318949	0.861385	2.341488
$a/h = 1.0$	1.248453	3.393648	1.958586	1.234958	3.356964

As it is seen from Eq. (1.1), the top of the layer becomes stiffer if the non-homogeneity parameter β increases or vice versa. Similarly, it can be observed from Eq. (1.2) that the top of the layer becomes heavier if the non-homogeneity parameter α increases. In addition, the layer can be assumed as homogenous for the non-homogeneity parameters $\beta = 0.001$ and $\alpha = 0.001$.

Note that all quantities are normalized. The height of the graded layer h is taken as 1, whereas Poisson's ratio of the graded layer is taken as 0.25. In addition, the iterations are continued until the accuracy is less than 10^{-6} for $N = 20$.

Table 1 shows the comparison of the critical load factor λ_{cr} in case of continuous contact and half separation distance b/h in case of discontinuous contact for a homogenous layer, *i.e.* $\beta = 0.001$ and $\alpha = 0.001$, between the values reported in Civelek and Erdogan [1] and obtained in this study. It can be seen that the λ_{cr} and b/h values of this study are approximately the same values as given by Civelek and Erdogan [1].

Tables 2 and 3 show the variation of the critical load factor λ_{cr} for various non-homogeneity parameters β, α, and uniformly distributed load amplitude a/h in case of continuous contact. It is seen from these Tables that λ_{cr} increases for increasing α if others are fixed. Similarly, increasing β results in an increment of the load factor λ_{cr}. In addition, λ_{cr} increases for increasing a/h. The smallest critical load needed to separate the FG layer from the rigid foundation is obtained in case of a concentrated load, *i.e.*, $a/h = 0.01$.

The effect of the load factor λ, non-homogeneity parameters β and α, and uniformly distributed load magnitude a/h on the contact pressure in case of continuous contact are shown in Figs. 3, 4, and 5, respectively. It can be seen from these Figures that the lowest pressure occurs on the symmetry axis and pressure becomes zero for the critical load factor. In addition, the effect of the loading decreases moving away from the symmetry axis and goes to a definite value that represents the particular solution of stress given in (10) and changes with mass density, *i.e.*, ρ_0 and α.

In case of discontinuous contact, the comparison of the half separation distance b/h and the accuracy, *i.e.*, the difference between the left-hand side and right-hand side of the $(N/2+1)th$ equation of (43), in each step of the iterative procedure described at the end of Sect. 4 for various non-homogeneity parameters α and β is given in Table 4. As it is seen from the Table, iterations are continued until the absolute value of accuracy is less than 10^{-6}, and at most 17 iterations are required to solve the problem.

Tables 5 and 6 show the variation of half contact distance b/h between the FG layer and the rigid foundation for various non-homogeneity parameters β,α and uniformly distributed load amplitude a/h in case of discontinuous contact for a constant load factor, λ. It can be seen from the Tables that b/h decreases with

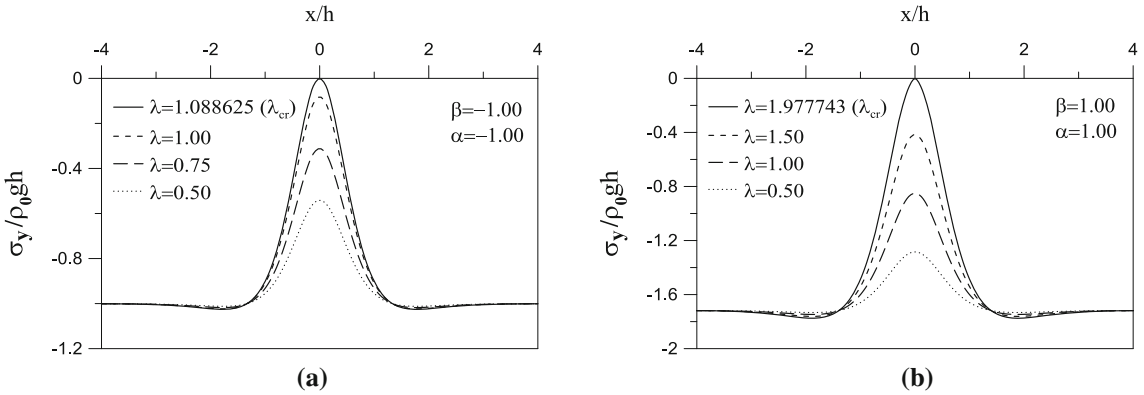

Fig. 3 The effect of λ on the contact pressure for various β and α in case of continuous contact ($a/h = 0.01, \kappa = 2.0$)

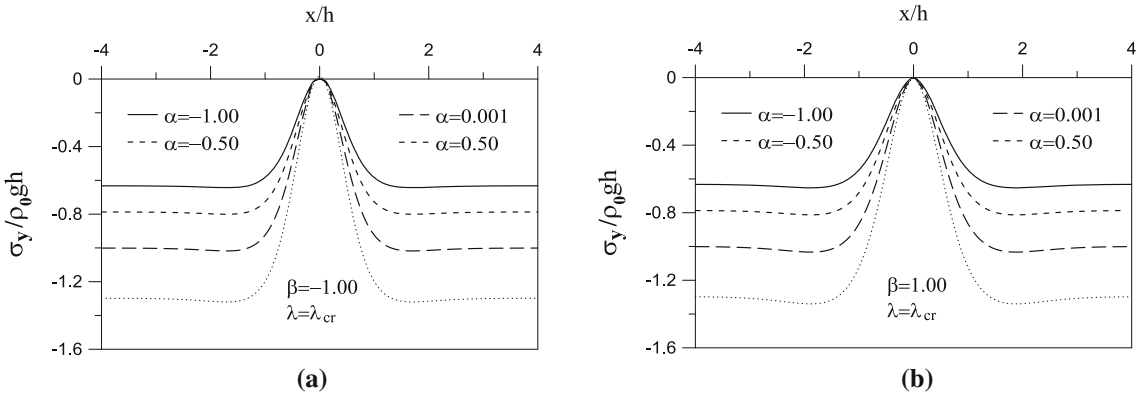

Fig. 4 The effect of β and α on the contact pressure for $\lambda = \lambda_{cr}$ in case of continuous contact ($a/h = 0.01, \kappa = 2.0$)

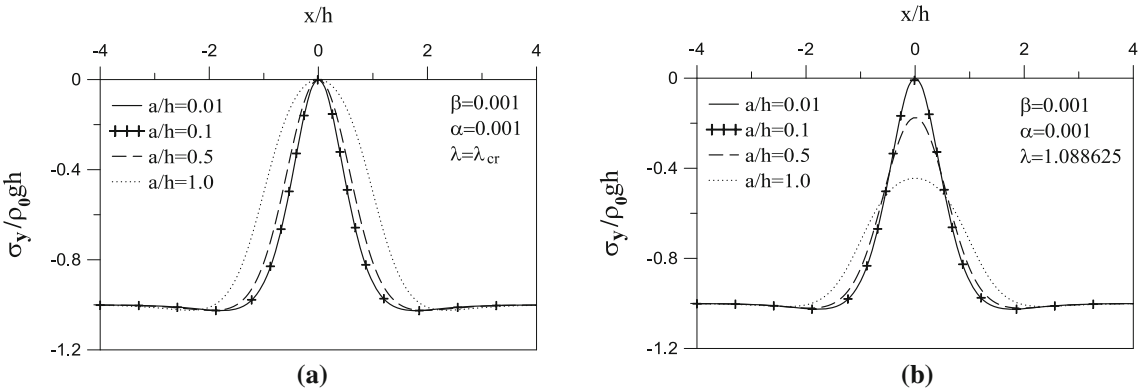

Fig. 5 The effect of a/h on the contact pressure for various β and α in case of continuous contact ($\kappa = 2.0$)

increasing β for a fixed value of α. Similarly, increasing α results in a reduction of the half separation distance. In addition, b/h decreases with increasing a/h, and the largest separation distance is obtained in case of concentrated load, *i.e.*, $a/h = 0.01$ independent of β and α.

The effect of the load factor λ, non-homogeneity parameters β and α, and uniformly distributed load magnitude a/h on the contact pressure in case of discontinuous contact are shown in Figs. 7 and 8, respectively. Similar to the continuous contact case, the effect of the loading decreases moving away from the symmetry axis and goes to a definite value that represents the particular solution of stress given in (10) and changes with mass density, *i.e.* ρ_0 and α. It can be seen from these Figures that the largest pressures occur near the end of the separation. Moreover, they increase for increasing α, β, and λ while decrease for increasing a/h.

Table 4 The variation of b/h and accuracy at each iteration for various non-homogeneity parameters β and α in case of discontinuous contact ($a/h = 0.01$)

$\beta = -1.0, \alpha = -1.0$			$\beta = 0.001, \alpha = 1.0$			$\beta = 1.0, \alpha = 0.001$		
Iter. no.	b/h	Accuracy	Iter. no.	b/h	Accuracy	Iter. no.	b/h	Accuracy
1	0.200000	56.256269	1	0.200000	35.835082	1	0.200000	50.680951
2	1.055712	16.615551	2	0.941528	4.177409	2	1.306197	7.551998
3	1.853711	7.009563	3	1.136343	0.65902	3	1.882285	2.337714
4	2.888897	2.545519	4	1.180796	0.01923	4	2.260852	0.385044
5	3.839936	0.731954	5	1.182199	−0.000069	5	2.351033	0.013114
6	4.415509	0.171781	6	1.182194	−0.000085	6	2.354353	0.010459
7	4.670349	0.031045	…	……	……	7	2.356450	−0.008331
8	4.744432	0.002647	14	1.182189	−0.000008	8	2.354332	0.000032
9	4.751762	−0.000035	15	1.182189	0.000067	9	2.354342	0.000005
10	4.751655	0.000004	16	1.182194	−0.000109	10	2.354344	0.000000
11	4.751669	0.000000	17	1.182186	0.000000			

Table 5 The variation of b/h for the various non-homogeneity parameters β and α in case of discontinuous contact ($a/h = 0.01$, $\lambda = 4$)

Parameters	$\alpha = -1.0$	$\alpha = -0.5$	$\alpha = 0.001$	$\alpha = 0.5$	$\alpha = 1.0$
$\beta = -1.0$	4.751669	3.308814	2.436338	1.751601	1.208481
$\beta = -0.5$	4.238259	3.226682	2.406783	1.735233	1.195486
$\beta = 0.001$	4.115861	3.186628	2.387936	1.721536	1.182186
$\beta = 0.5$	4.042882	3.156730	2.371358	1.707880	1.167690
$\beta = 1.0$	3.985572	3.129293	2.354350	1.693083	1.151203

Table 6 The variation of b/h for various a/h, non-homogeneity parameters β and α in case of discontinuous contact ($\lambda = 4$)

Parameters	$\beta = -1.0$ $\alpha = -1.0$	$\beta = -1.0$ $\alpha = 1.0$	$\beta = 0.001$ $\alpha = 0.001$	$\beta = 1.0$ $\alpha = -1.0$	$\beta = 1.0$ $\alpha = 1.0$
$a/h = 0.01$	4.751669	1.208481	2.387936	3.988572	1.167690
$a/h = 0.1$	4.733200	1.206925	2.386910	3.984403	1.149657
$a/h = 0.5$	4.578875	1.165827	2.362005	3.967299	1.108694
$a/h = 1.0$	4.454754	0.926750	2.278638	3.924370	0.877039

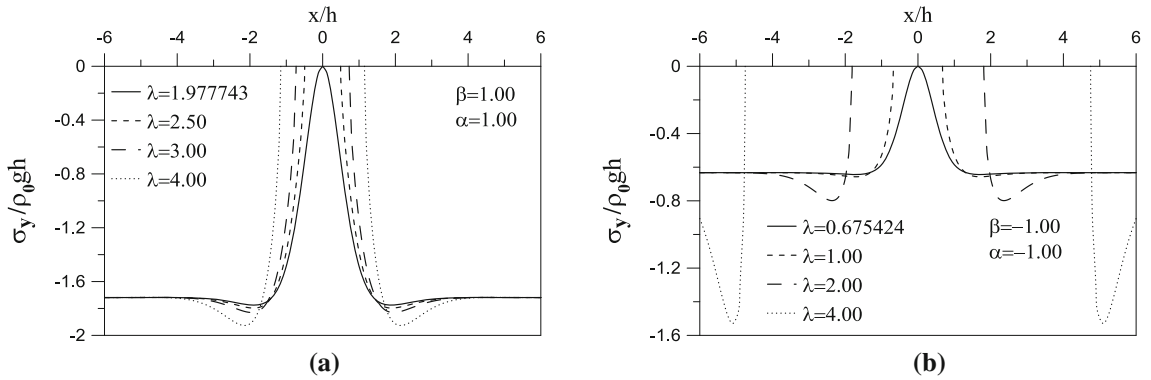

Fig. 6 The effect of λ on the contact pressure for various β and α in case of discontinuous contact ($a/h = 0.01, \kappa = 2.0$)

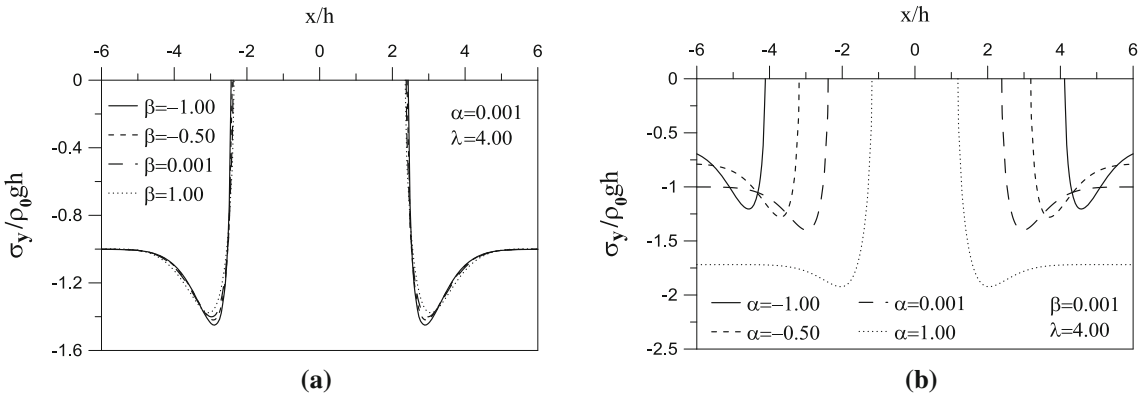

Fig. 7 The effect of β and α on the contact pressure in case of discontinuous contact ($a/h = 0.01$, $\kappa = 2.0$)

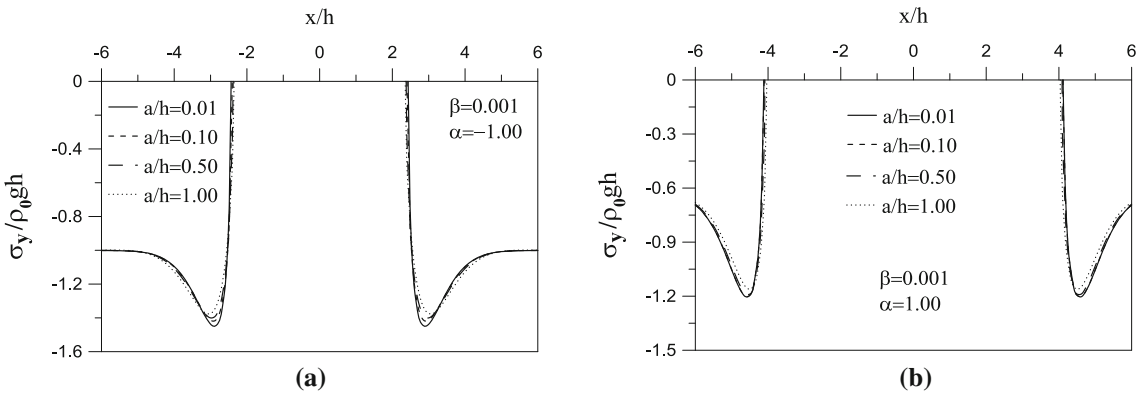

Fig. 8 The effect of a/h on the contact pressure for various β and α in case of discontinuous contact ($\lambda = 4.0$, $\kappa = 2.0$)

6 Conclusions

In this paper, the continuous and discontinuous contact problem of a functionally graded (FG) layer resting on a rigid foundation was considered. The top of the FG layer is subjected to normal tractions over a finite segment. The calculations were made under the assumption that the FG layer is isotropic and the shear modulus and mass density vary exponentially along the direction of the layer's thickness.

For continuous contact, the problem was solved analytically using plane elasticity and integral transform techniques. The critical load that causes first separation and contact pressures was investigated for various material properties and loadings. It was seen that the critical load increased with increasing non-homogeneity parameters β, α, and distributed load amplitude a/h. In addition, the lowest pressure occurred on the symmetry axis.

For discontinuous contact, the problem reduced to a singular integral equation using plane elasticity and integral transform techniques. The obtained singular integral equation was solved numerically using Gauss–Jacobi integration formulation, and an iterative scheme was employed to obtain the correct separation distance. The effect of the non-homogeneity parameters β, α, and loading on the separation distance and on the contact pressure were investigated using a parametric study. It was seen that the separation distance decreased with increasing non-homogeneity parameters β, α, and distributed load amplitude. In addition, the largest pressures occur near the end of the separation and increase for increasing α while decrease for increasing β.

It was also seen that the effect of the loading decreased moving away from the symmetry axis and went to a definite value that represents the particular solution of stress given in (10) and changes with mass density, *i.e.*, ρ_0 and α.

Appendix A

F_{j1} $(j = 1, \ldots, 4)$ and ΔF in case of continuous contact are defined as follows:

$$F_{11} = \exp(n_2 h)\,(T_2T_3m_4 - T_2T_4m_3) + \exp(n_3 h)\,(-T_2T_3m_4 + T_3T_4m_2) + \exp(n_4 h)\,(T_2T_4m_3 - T_3T_4m_2)\,, \tag{A1}$$

$$F_{21} = -\exp(n_1 h)\,(T_1T_3m_4 - T_1T_4m_3) - \exp(n_3 h)\,(-T_1T_3m_4 + T_3T_4m_1) - \exp(n_4 h)\,(T_1T_4m_3 - T_3T_4m_1)\,, \tag{A2}$$

$$F_{31} = \exp(n_1 h)\,(T_1T_2m_4 - T_1T_4m_2) + \exp(n_2 h)\,(-T_1T_2m_4 + T_2T_4m_4) + \exp(n_4 h)\,(T_1T_4m_2 - T_2T_4m_1)\,, \tag{A3}$$

$$F_{41} = -\exp(n_1 h)\,(T_1T_2m_3 - T_1T_3m_2) - \exp(n_2 h)\,(-T_1T_2m_3 + T_2T_3m_1) - \exp(n_3 h)\,(T_1T_3m_2 - T_2T_3m_1)\,, \tag{A4}$$

$$\begin{aligned}\Delta F = {} & \exp((n_1+n_2)h)\,(\ S_1T_2T_3m_4 - S_1T_2T_4m_3 - S_2T_1T_3m_4 + S_2T_1T_4m_3)\\ & \exp((n_1+n_3)h)\,(-S_1T_2T_3m_4 + S_1T_3T_4m_2 + S_3T_1T_2m_4 - S_3T_1T_4m_2)\\ & \exp((n_1+n_4)h)\,(\ S_1T_2T_4m_3 - S_1T_3T_4m_2 - S_4T_1T_3m_2 + S_4T_1T_3m_2)\\ & \exp((n_2+n_3)h)\,(\ S_2T_1T_3m_4 - S_2T_3T_4m_1 - S_3T_1T_2m_4 + S_3T_2T_4m_1)\\ & \exp((n_2+n_4)h)\,(-S_1T_2T_4m_3 + S_2T_3T_4m_1 + S_4T_1T_2m_3 - S_4T_2T_3m_1)\\ & \exp((n_3+n_4)h)\,(\ S_3T_1T_2m_4 - S_3T_2T_4m_1 - S_4T_1T_3m_2 + S_4T_2T_3m_1)\,.\end{aligned} \tag{A5}$$

F_{j1}, F_{j2} $(j = 1, \ldots, 4)$ and ΔF in case of discontinuous contact are defined as follows:

$$\begin{aligned}\mathrm{F}_{11} = {} & \exp((n_2+n_3)h)\,(S_2T_3T_4 - S_3T_2T_4) + \exp((n_2+n_4)h)\,(-S_2T_3T_4 + S_4T_2T_3)\\ & + \exp((n_3+n_4)h)\,(\ S_3T_2T_4 - S_4T_2T_3)\,,\end{aligned} \tag{A6}$$

$$\begin{aligned}\mathrm{F}_{21} = {} & \exp((n_1+n_3)h)\,(S_3T_1T_4 - S_1T_3T_4) + \exp((n_1+n_4)h)\,(S_1T_3T_4 - S_4T_1T_3)\\ & + \exp((n_3+n_4)h)\,(-S_3T_1T_4 - S_4T_1T_3)\,,\end{aligned} \tag{A7}$$

$$\begin{aligned}\mathrm{F}_{31} = {} & \exp((n_1+n_2)h)\,(S_1T_2T_4 - S_2T_1T_4) + \exp((n_1+n_4)h)\,(-S_1T_2T_4 + S_4T_1T_2)\\ & + \exp((n_2+n_4)h)\,(S_2T_1T_4 - S_4T_1T_2)\,,\end{aligned} \tag{A8}$$

$$\begin{aligned}\mathrm{F}_{41} = {} & \exp((n_1+n_2)h)\,(S_2T_1T_3 - S_1T_2T_3) + \exp((n_1+n_3)h)\,(S_1T_2T_3 - S_3T_1T_2)\\ & + \exp((n_2+n_3)h)\,(-S_2T_1T_3 + S_3T_1T_2)\,,\end{aligned} \tag{A9}$$

$$\begin{aligned}\mathrm{F}_{12} = {} & \exp(n_2h)\,(T_1T_3m_4 - T_2T_4m_3) + \exp(n_3h)\,(-T_2T_3m_4 + T_3T_4m_2)\\ & + \exp(n_4h)\,(T_2T_4m_3 - T_3T_4m_2)\,,\end{aligned} \tag{A10}$$

$$\begin{aligned}\mathrm{F}_{22} = {} & \exp(n_1h)\,(T_2T_3m_4 - T_2T_4m_3) + \exp(n_3h)\,(-T_2T_3m_4 + T_3T_4m_2)\\ & + \exp(n_4h)\,(T_2T_4m_3 - T_3T_4m_2)\,,\end{aligned} \tag{A11}$$

$$\begin{aligned}\mathrm{F}_{32} = {} & \exp(n_1h)\,(T_1T_2m_4 - T_1T_4m_2) + \exp(n_2h)\,(-T_1T_2m_3 + T_2T_4m_1)\\ & + \exp(n_4h)\,(T_1T_4m_2 - T_2T_4m_1)\,,\end{aligned} \tag{A12}$$

$$\begin{aligned}\mathrm{F}_{42} = {} & \exp(n_4h)\,(T_1T_3m_2 - T_1T_2m_3) + \exp(n_2h)\,(T_1T_2m_3 - T_2T_3m_1)\\ & + \exp(n_3h)\,(-T_1T_3m_2 + T_2T_3m_1)\,,\end{aligned} \tag{A13}$$

$$\begin{aligned}\Delta F = {} & \exp((n_1+n_2)h)\,\xi\,(\ S_1T_2T_3m_4 - S_1T_2T_4m_3 - S_2T_1T_3m_4 + S_2T_1T_4m_3)\\ & \exp((n_1+n_3)h)\,\xi\,(-S_1T_2T_3m_4 + S_1T_3T_4m_2 + S_3T_1T_2m_4 - S_3T_1T_4m_2)\\ & \exp((n_1+n_4)h)\,\xi\,(\ S_1T_2T_4m_3 - S_1T_3T_4m_2 - S_4T_1T_2m_3 + S_4T_1T_3m_2)\\ & \exp((n_2+n_3)h)\,\xi\,(\ S_2T_1T_3m_4 - S_2T_3T_4m_1 - S_3T_1T_2m_4 + S_3T_2T_4m_1)\\ & \exp((n_2+n_4)h)\,\xi\,(-S_2T_1T_4m_3 + S_2T_3T_4m_1 + S_4T_1T_2m_3 - S_4T_2T_3m_1)\\ & \exp((n_3+n_4)h)\,\xi\,(\ S_3T_1T_4m_2 - S_3T_2T_4m_1 - S_4T_1T_3m_2 + S_4T_2T_3m_1)\,.\end{aligned} \tag{A14}$$

K_1 and K_2 in (35) are defined as follows:

$$K_1 = \int_0^\infty \frac{\kappa+1}{4}\left[K_1^* - K_{1s}\right]\sin\xi\,(t-x)\,d\xi, \tag{A15.1}$$

$$K_2 = \int_0^\infty \sum_{j=1}^{4} \frac{1}{\Delta F} F_{j2} S_j \sin \xi a \cos \xi x d\xi \tag{A15.2}$$

in which K_{1s} represents the first asymptotic term of K_1^*, and they are defined as follows:

$$K_1^* = \frac{1}{\kappa - 1} \sum_{j=1}^{4} \frac{1}{\Delta F} F_{j1} S_j, \tag{A16.1}$$

$$K_{1s} = \frac{4}{\kappa + 1}, \tag{A16.2}$$

r_i and s_k in (43) are defined as follows:

$$s_j = \cos \frac{j\pi}{N+1}, \qquad j = 1, \ldots, N, \tag{A17}$$

$$r_i = \cos \frac{(2i-1)\pi}{2(N+1)}, \qquad i = 1, \ldots, N+1. \tag{A18}$$

References

1. Civelek, M.B., Erdogan, F.: Frictionless contact problem for an elastic layer under gravity. J. Appl. Mech. Trans. ASME **42**, 136–140 (1975)
2. Civelek, M.B., Erdogan, F., Cakiroglu, A.O.: Interface separation for an elastic layer loaded by a rigid stamp. Int. J. Eng. Sci. **16**, 669–679 (1978)
3. Cakiroglu, A.O., Cakiroglu, F.L.: Continuous and discontinuous contact problems for strips on an elastic semi-infinite plane. Int. J. Eng. Sci. **29**, 99–111 (1991)
4. Birinci, A., Erdol, R.: A frictionless contact problem for two elastic layers supported by a Winkler foundation. Struct. Eng. Mech. **15**, 331–344 (2003)
5. Oner, E., Birinci, A.: Continuous contact problem for two elastic layers resting on an elastic half-infinite plane. J. Mech. Mater. Struct. **9**, 105–119 (2014)
6. Birinci, A., Adiyaman, G., Yaylaci, M., Oner, E.: Analysis of continuous and discontinuous cases of a contact problem using analytical method and FEM. Lat. Am. J. Solids Struct. **12**, 1771–1789 (2015)
7. Giannakopoulos, A.E., Pallot, P.: Two-dimensional contact analysis of elastic graded materials. J. Mech. Phys. Solids. **48**, 1597–1631 (2000)
8. Guler, M.A., Erdogan, F.: Contact mechanics of graded coatings. Int. J. Solids Struct. **41**, 3865–3889 (2004)
9. Guler, M.A., Erdogan, F.: Contact mechanics of two deformable elastic solids with graded coatings. Mech. Mater. **38**, 633–647 (2006)
10. Ke, L.L., Wang, Y.S.: Two-dimensional sliding frictional contact of functionally graded materials. Eur. J. Mech. A-Solid. **26**, 171–188 (2007)
11. Barik, S.P., Kanoria, M., Chaudhuri, P.K.: Steady state thermoelastic contact problem in a functionally graded material. Int. J. Eng. Sci. **46**, 775–789 (2008)
12. Ke, L.L., Yang, J., Kitipornchai, S., Wang, Y.S.: Electro-mechanical frictionless contact behavior of a functionally graded piezoelectric layered half-plane under a rigid punch. Int. J. Solids Struct. **45**, 3313–3333 (2008)
13. Dag, S., Guler, M.A., Yidirim, B., Ozatag, A.C.: Sliding frictional contact between a rigid punch and a laterally graded elastic medium. Int. J. Solids Struct. **46**, 4038–4053 (2009)
14. Comez, I.: Contact problem of a functionally graded layer resting on a Winkler foundation. Acta Mech. **224**, 2833–2843 (2013)
15. Comez, I.: Contact problem for a functionally graded layer indented by a moving punch. Int. J. Mech. Sci. **100**, 339–344 (2015)
16. Krenev, L.I., Aizikovich, S.M., Tokovyy, Y.V., Wang, Y.C.: Axisymmetric problem on the indentation of a hot circular punch into an arbitrarily nonhomogeneous half-space. Int. J. Solids Struct. **59**, 18–28 (2015)
17. Wang, Z.J., Yu, C.J., Wang, Q.: An efficient method for solving three-dimensional fretting contact problems involving multilayered or functionally graded materials. Int. J. Solids Struct. **66**, 46–61 (2015)
18. Parel, K.S., Hills, D.A.: Frictional receding contact analysis of a layer on a half-plane subjected to semi-infinite surface pressure. Int. J. Mech. Sci. **108**, 137–143 (2016)
19. Ma, J., El-Borgi, S., Ke, L.L., Wang, Y.S.: Frictional contact problem between a functionally graded magnetoelectroelastic layer and a rigid conducting flat punch with frictional heat generation. J. Therm. Stress. **39**, 245–277 (2016)
20. El-Borgi, S., Abdelmoula, R., Keer, L.: A receding contact plane problem between a functionally graded layer and a homogeneous substrate. Int. J. Solids Struct. **43**, 658–674 (2006)

21. Rhimi, M., El-Borgi, S., Ben Said, W., Ben Jemaa, F.: A receding contact axisymmetric problem between a functionally graded layer and a homogeneous substrate. Int. J. Solids Struct. **46**, 3633–3642 (2009)
22. Rhimi, M., El-Borgi, S., Lajnef, N.: A double receding contact axisymmetric problem between a functionally graded layer and a homogeneous substrate. Mech. Mater. **43**, 787–798 (2011)
23. Yang, J., Ke, L.L.: Two-dimensional contact problem for a coating-graded layer-substrate structure under a rigid cylindrical punch. Int. J. Mech. Sci. **50**, 985–994 (2008)
24. Chen, P.J., Chen, S.H.: Contact behaviors of a rigid punch and a homogeneous half-space coated with a graded layer. Acta Mech. **223**, 563–577 (2012)
25. El-Borgi, S., Usman, S., Guler, M.A.: A frictional receding contact plane problem between a functionally graded layer and a homogeneous substrate. Int. J. Solids Struct. **51**, 4462–4476 (2014)
26. Yan, J., Li, X.: Double receding contact plane problem between a functionally graded layer and an elastic layer. Eur. J. Mech. A-Solid. **53**, 143–150 (2015)
27. Kulchytsky-Zhyhailo, R., Bajkowski, A.S.: Three-dimensional analytical elasticity solution for loaded functionally graded coated half-space. Mech. Res. Commun. **65**, 43–50 (2015)
28. Alinia, Y., Beheshti, A., Guler, M.A., El-Borgi, S., Polycarpou, A.A.: Sliding contact analysis of functionally graded coating/substrate system. Mech. Mater. **94**, 142–155 (2016)
29. Erdogan, F., Gupta, G.D.: Numerical solution of singular integral-equations. Q. Appl. Math. **29**, 525 (1972)